The final publication is available at Springer via http://dx.doi.org/10.1007/s12247-014-9206-1

Loss-in-Weight Feeding Trials Case Study: Pharmaceutical Formulation

Abstract: This article presents a case study of a continuous feeding strategy for five pharmaceutical components (API, Prosolv HD90, Crospovidone, Magnesium Stearate, and Colloidal Silicon Dioxide), for the purpose of developing a direct compression continuous manufacturing system. Feeding options for each of these five powders were examined. Prosolv HD90 and Crospovidone easily resulted in optimal feeding conditions, whereas the remaining powders in the formulation presented some challenges. The API displayed flow issues, leading to clogging of the screen with small openings. Magnesium stearate exhibited shear sensitivity; increasing shear of the powder due to hopper agitation resulted in drifting feeding performance. Colloidal silicon dioxide exhibited electrostatic issues that render most tooling options unsuitable for steady operation. All of these difficulties were resolved using the methods described in this article.

1 Introduction

While the great majority of pharmaceutical products are produced through batch manufacturing, recent years have witnessed a growing interest in continuous manufacturing methods. Relative to other industries, the pharmaceutical industry has been slow in adopting modern manufacturing approaches, often citing regulatory uncertainty [1], [2] as the main reason. However, in recent years, industry and academia have engaged in many studies to demonstrate the benefits of continuous manufacturing processes and to create reliable methods for their design, optimization, and control. [1], [3]–[11]

One of the key issues in powder-based continuous manufacturing is the need to feed accurately poorly flowing raw ingredients at the ratios needed for a given formulation. In a continuous system, if the feed rate of one ingredient changes even for a brief period of time, the resulting perturbation in concentration of the process stream will propagate

downstream [12]–[15], potentially leading to out of specification product units. Hence, the ability to feed powder consistently and continuously is often regarded as one of the critical requirements of the overall process. While for large scales of operation and for freely-flowing powders (i.e., most granulations) this is generally not a difficult feat, at the small flowrates associated with typical pharmaceutical processes (0.5-100 Kg/hr), inaccuracies in feeding rates of dispensed component feedstreams need to be carefully addressed and minimized.

Singh *et al* [8], [16] describes a flexible multifunction continuous manufacturing platform (being developed at the ERC-SOPS) which aims to provide side-by-side the multiple processing routes for the continuous manufacturing of tablets: direct compaction (DC), wet granulation (WG), and dry granulation (DG). In this article, we are primarily interested in direct compression, where the powders are fed, blended, and compressed into tablets without a granulation step. The feeding process is the same among all processing routes. A typical direct compression process, adapted for continuous manufacturing, is shown in Figure 1. The overall process for the formulation consists of 4 main unit operations: feeding, delumping (milling), blending, and compaction. As shown in Figure 1, feeding is the first step and consists of several different feeders. Variations and inaccuracies at this step are magnified and complicated by the number of feeders used.

Although the feeders are typically different for each ingredient, the principle of operation and the general components of the feeders are the same. Every loss-in-weight feeder consists of three parts [17], [18]: volumetric feeder, weighing platform (load cell), and gravimetric controller (see Figure 2). The volumetric feeder is mounted on top of a

weighing platform that measures the mass of the feeder and its powder contents. The most common mechanism that the volumetric feeder uses to dispense the powder includes: screw [19], vibration [20], belt [21], and rotary valve [22]. Regardless of type, the theory of gravimetric loss-in-weight control and the function of the feeder remains the same. For this case study, all of the feeders were of the most common screw-driven type.

Under normal operation, a loss-in-weight feeder operates in gravimetric control mode. This means that as the feeder dispenses powder, the gravimetric controller acquires a signal from the loadcell in the weighing platform as a function of time. Using the change in weight measured over time, the controller can determine the instantaneous feedrate, which is compared to the desired setpoint. The feedrate is then controlled by adjusting the screw speed, which determines the rate at which powder is dispensed from the feeder.

Alternatively, the feeders can operate in a volumetric mode, where the screw speed is kept constant and a predefined calibration variable, called the "feed factor", is used to determine screw speed based on a setpoint. The "feed factor" is the gravimetric speed equivalent for 100% screw speed [23]. Feeder manufacturers will use a different term for this value although the general meaning and function remains the same. The volumetric mode is not optimal, as it does not adjust for variations in density that typically occur when emptying and refilling the hopper [24]; however, it is necessary when gravimetric control mode is not possible, such as during startup and hopper refill.

In this work, a case study is presented, where a commercial formulation is investigated in order to develop a feeding regime that enables a continuous manufacturing process. As the optimal feeding configuration (tooling selection) for any powder is based on both

feedrate and powder properties, it is important to rigorously test and investigate each component separately. This involves determining the constraints in feeder and feeding tooling for each individual component in the formulation, testing potentially successful configurations, and comparing the feeding performance between the different configurations. This ensures that when the components are fed simultaneously, the resulting feed streams will combine with minimal fluctuations in the ratios required by the formulation.

The optimized feeding regime was determined for a formulation containing the following components: a proprietary active pharmaceutical ingredient (API), Prosolv HD90, crosspovidone, magnesium stearate, and silicon dioxide. Feeding configurations for Prosolv HD90 and crosspovidone were optimized with minimal difficulty, mainly due to their free-flowing behavior. The API, although relatively free-flowing, had some tendencies to clog in discharge screens, which caused it to be incompatible with several of the smaller aperture screens. Magnesium stearate presented some challenges due to its shear sensitivity and its tendency to coat metal tooling. Silicon dioxide had issues with adhesion due to its light density and strong electrostatic behavior. These problems were successfully addressed, as explained below. Although the results presented here are formulation specific, the approach used is applicable to any formulation.

2 Equipment

2.1 Feeders

The feeders used in these feeding trials are the KT35, KT20, and MT12 (See Figure 2 and Table 1) by K-Tron (Sewell, NJ). All of these feeders are based on gravimetric control

principles and use loss-in-weight data to control the feedrate. They are all twin-screw feeders, consisting of a twin-screw driven feeder mounted on a weigh bridge. For each feeder, there are several feeding screws and discharge screens available (see Figure 3), allowing the feeding of bulk powder materials with a large range of cohesions at a wide range of feedrates. Although there are multiple methods for improving feeding performance through feeder modification [25], [26], only standard tooling available through the feeder manufacturer was used in this study.

Each feeder has a different set of tooling that is only compatible with that feeder type and size. Each of the feeders has their own set of 4 different twin screws: coarse concave (CCS), coarse auger (CAS), fine concave (FAS), and fine auger (FAS). Each of these screws is specific to a single feeder model, as each has a different diameter: 35mm for the KT35, 20mm for the KT20, and 12mm for the MT12. Coarse and fine screws have different capacities, which are determined by the size of the pockets created by the pitch of the screws. The concave screws have a "self-cleaning" function, which is useful when feeding "sticky" powders that will otherwise adhere to the metal tooling, reducing throughput and performance. The auger screws do not have this "self-cleaning" ability, but have the advantage of higher capacity.

Each feeder has multiple discharge screens that can be paired with the different sets of screws (see Table 2). The K-Tron KT35 has 3 screen conditions: coarse square screen (CSqS), fine square screen (FSqS), and no screen (NoS). The K-Tron KT20 has 4 screen conditions: coarse square screen (CSqS), medium square screen (MSqS), fine square screen (FSqS), and no screen (NoS). The K-Tron MT12 has 5 screen conditions: Coarse Square Screen (CSqS), Fine Square Screen (FSqS), Coarse Slotted Screen (CSlS), Fine

Slotted Screen (FSlS) and No Screen (NoS). The function of the screens is two-fold. They can be used to break up clumps for cohesive powders, and can also be used for very free-flowing powders to create back-pressure that holds the material from freely flowing from the feeder.

2.2 Catch Scale

As described in a previous manuscript [27], a Schenck Accurate AccPro II "catch scale" was used to characterize feeder performance. This was the same system described in the previous manuscript. The notable difference was a 1 kg strain gage loadcell was added to measure the very small feedrates of the K-Tron MT12. For the larger feedrates of the K-Tron KT20 and KT35, the 7 kg strain gage loadcell was still used. The use of a catch scale removes the bias associated with using the internal loadcell of a gravimetric feeder, thereby allowing accurate comparison between different feeders.

3 Method for characterizing gravimetrically controlled feeding performance

The steady state feeding performance of each feeder was evaluated using the relative standard deviation index. This information can be used to select the best feeder tooling for a given powder at a given feedrate. Characterization experiments were conducted using the catch scale to record the weight of powder delivered by the feeder at the highest resolution possible of the catch scale. The method has been extensively detailed in a previous publication [27]. The main difference in the feeder characterization method is the range of setpoints that were used. The desired setpoints to be tested depend on the reason for testing. If testing is performed to determine the limits of the feeder for a given powder, the rates may be set on the entire screw speed range of the feeder, such as: 10%,

20%, 50%, 80%, 90% and 100% of the overall screw speed. The corresponding gravimetric setpoints are determined through volumetric testing at each of these screw speeds. Alternatively, and in the case of this study, the feedrate setpoints are defined by the ranges required for the throughput capacities of the formulation: 80%, 100% and 125% of the nominal capacity of 30 kg/hr.

The feeders were mounted on a sturdy surface and the catch scale was placed on a separate lower stand, effectively isolating the catch scale from any vibrations that might emanate from the feeder. If and when the container on the scale became full, it was replaced by an empty one. Data collection was "paused" during this contained exchange so that this disturbance did not affect the results. Due to the sensitivity of the load cells in the equipment, careful consideration was taken to isolate and minimize outside disturbances on the feeders and catch scale. In addition, samples were taken to test for the effect of feeding on the powders. The powder samples were used to investigate for potential changes to powder properties in a Freeman Technology FT4 powder testing system using the compressibility and shear cell tests.

3.1 General Procedure

The general procedure for the characterization experiments is as follows:

1. Calibrate the load cells in the feeder and catch scale.
2. Fill the feeder to 100% of the maximum fill level.
3. Find maximum feed rate for each experimental combination, and use this value for the initial feed factor controller value.
4. Run feeding trials at desired setpoints starting at the maximum fill level.

The initial calibration of the feeder and catch scale load cells is of utmost importance, because if either of these are miscalibrated then the values collected from these load cells would be meaningless. Miscalibration of the feeder load cell has an additional implication since the feeder uses this signal for control. If this is incorrect, the feeder will misinterpret changes in weight, thus controlling to a different value than setpoint. This is a common mistake made when the wrong units are used for a check weight. This can be quite confusing to an operator that enters a desired setpoint of 5 kg/hr which is then displayed on the controls of the feeder, yet the actual feedrate being fed is 5 lbs/hr (or 2.27 kg/hr). Unless checked with a correctly calibrated catch scale, or until the calibration is rechecked with a check weight, it may go unnoticed until problems are discovered downstream.

The initial filling of the feeder is important as there is often a substantial change in the screw filling at lower fill levels. To avoid this issue altogether, it is recommended to fill the feeder to close to maximum for testing, thereby ensuring that the minimum operation level is exceeded. Most feeding manufacturers state that this minimum is ~20% hopper fill level, but this is dependent on powder properties and may vary.

The maximum feed rate is found by running the feeder in volumetric mode at the maximum 100% screw speed. Alternatively, this value can be obtained at a lower speed through extrapolation, which is commonly a preset function created by the manufacturers and accessible through the program menus of the feeder. This is advantageous in that it conserves powder, but it is also not as robust as a direct test and may cause problems if the relationship between screw speed and powder feedrate is not linear. Although this is not very common for free flowing powders, it becomes more common with powders that

are cohesive and are unable to consistently fill the flights of the screw at higher rotation rates.

3.2 Analysis

The raw data from the catch scales was extracted using the Excel export option from the catch scale software package. To analyze the data, the powder exiting the feeder was collected over a period of 1 second and its mass was used to calculate the fed material mass for the interval. From all the mass flowrates at each interval a distribution can be created, and the standard deviation (σ) and relative standard deviation (RSD) can be calculated. After modest filtering to remove irrelevant disturbances (as described in detail in the previous publication [27]), the standard deviation and the average feedrate was calculated and used for comparison of feeding performance for the different data sets.

Unless there are very large oscillations, the distributions of feedrate from the feeders have a near Gaussian distribution like the one shown in Figure 4b. Significant uniform oscillations would result in a distribution that is more 'U' shaped. Figure 5b shows the resulting distribution created from large oscillations in feedrate (Figure 5a) which can be compared to a sine wave function (Figure 5c) and its characteristic 'U' shaped distribution (Figure 5d). As this is non-optimal operation of the feeders and may lead to process instabilities, it should be avoided when possible.

4 Conditions examined in this study

The throughput requirements for each powder are directly related to the powder formulation, which is shown in Table 3. The nominal overall set point feedrate for the

process studied here is 30 kg/hr. The range of interest for the feeding trials is 80% to 125% of this nominal formulation throughput. Using these values and the formulation feedrate, ranges for each component can be easily calculated. Although the feeders are often capable of much larger ranges, the range of 80% to 125% of the nominal formulation throughput was chosen such that the performance measured is maximally relevant to the formulation of interest under the conditions relevant to the actual manufacturing process. The target gravimetric feedrates were converted to corresponding volumetric feedrates based on approximate bulk densities. These volumetric feedrates were then compared with the volumetric capacities of the feeder and tooling configurations to narrow the choice of configurations to those feeders and tooling combinations that could potentially achieve the desired range of flows. These are potentially achievable configurations, because 100% screw flight filling is unlikely and this may reduce the overall throughput that is actually achievable with any specific tooling configuration. It is also important that any single tooling configuration can achieve the entire desired range of flows.

Testing of the feeding consistency was performed for 3 setpoints: nominal (100%), 80% and 125%. Using a nominal formulation throughput of 30 kg/hr, the following Table 4 shows the feedrates for each component to be tested. The bottom part of Table 4 shows the conversion from gravimetric feedrates (kg/hr) to approximate volumetric feedrates (dm^3/hr).

Assuming close to ideal filling of the screws, the appropriate feeder and screws for testing can be determined. The theoretical volumetric capacity for each feeder is shown in their respective Table 5-Table 7. The calculated volumetric feedrates for each powder

should be compared to the theoretical volumetric capacities of the feeders to determine potential feeding configurations that need to be tested. The volumetric capacity of any set of screws follows the equation:

$$\dot{v} = \omega * V_{rotation} * \varepsilon_{fill} \quad (1)$$

where ω is the rotation rate, $V_{rotation}$ is the volume dispensed per revolution, and ε_{fill} is the flight fill fraction. The fill fraction accounts for incomplete or non-ideal filling with powders that do not easily fill the flights of the screw. For ideally flowing powders, the fill fraction equals 1, meaning that the powder completely fills the volume of the flights in the screws.

An initial set of experiments was designed with the major components, Active Pharmaceutical Ingredient (API) and Prosolv HD90, being tested with the K-Tron KT20 and the minor components, Crospovidone and Magnesium Stearate, being tested with the K-Tron MT12.

4.1 ProSolv HD90

ProSolv HD90 is a high density silicified microcrystalline cellulose filler that promotes good flow and good compaction properties on a formulation for direct compression. In this formulation, it is the main excipient used, with a desired flowrate range from 10.64 kg/hr to 16.62 kg/hr (21.7 to 33.9 dm^3/hr), which falls on the upper end of the capacity of the K-Tron KT20, but on the lower end of the K-Tron KT35. This means that, assuming ideal flight filling of the screws, the powder flowrates can be achieved on both feeders. This excipient is very free flowing and the powder easily fills the flights of the screws. To feed at the upper end of the throughput of the KT20, both sets of the higher

throughput coarse screws were tested: coarse concave screws (CCS) and coarse auger screws (CAS). Both of the smaller throughput fine screws were deemed unable to achieve the high feedrates needed for ProSolv HD90 in this formulation. Four discharge screen conditions were available to be paired with each of the screws: coarse square screen (CSqS), medium square screen (MSqS), fine square screen (FSqS), and no screen (NoS).

For the feeding in the K-Tron KT35, the two fine sets of screws were used: fine concave screws (FCS) and fine auger screws (FAS). There are only two screens that can be used with the KT35, so there are three discharge screen conditions that were tested: coarse square screen (CSqS), fine square screen (FSqS), and no screen (NoS).

4.2 Active Pharmaceutical Ingredient (API)

Since this is a commercial product, the API identity is not disclosed here. The material is free-flowing with a particle size distribution with the following properties: d_{10} of 70 µm, d_{50} of 214 µm, and d_{90} of 447 µm. The desired flowrate range for API was 12.48 to 19.51 kg/hr (20.5 to 32 dm^3/hr), which once again fell on the upper range of the K-Tron KT20, but on the lower end of the K-Tron KT35. Therefore, both the coarse concave screws (CCS) and coarse auger screws (CAS) were appropriate for testing on the KT20. After some initial tests, it was found that the API material built up on the coarse auger screws, which can impact feeding performance, also creating traceability and maintenance concerns. From the throughput range of the CAS, it would appear that these screws would be able to handle this feeding task, but in practice this may not be the case, as the overall capacity will be reduced as the material adheres within the flights of the screws. In addition, stagnant material caught in the screws will have an extremely long

residence time, which may lead to material degradation and/or the need to clean the tooling very often. Thus, it was decided to use only self-cleaning screws to ensure that these stagnant zones and material buildup did not occur. The coarse concave screws were paired with all of the screen conditions of the KT20.

4.3 Colloidal Silicon Dioxide (Silica)

Colloidal silicon dioxide is a glidant that is used in low quantities to improve flow of the blend. Its low density, high cohesion, and electrostatics properties make it a very difficult material to handle as it will adhere to many surfaces and flows poorly. The desired flowrate range for colloidal silicon dioxide, 218 to 341 g/hr (5.5 to 8.5 dm^3/hr) falls in the mid to low range of the throughput of the K-Tron KT20. The ability of this powder to flow into the flights of the screws and fully fill them was unknown, but it was expected to be a challenge, so a broad range of tooling was initially screened for compatibility. All of the screens were found to be incompatible with the silica since the extra surfaces created extra buildup of silica at the feeder's discharge. The auger screws were also not an option as this could potentially lead to stagnant areas within the flights of the screws. The fine screws were unable to deliver the capacity needed for the entire desired feedrate range due to the material being unable to fully fill the flights of the screws. This left, as the only option for the K-Tron KT20 feeder, the coarse concave screws without a screen. The powder was also tested in the K-Tron KT35 with coarse concave screws, expecting that the larger feeder could improve flight filling consistency due to the use of much larger screws.

4.4 API and Silica Preblend

As explained above, preliminary testing of the colloidal silicon dioxide demonstrated that this material would adhere to screws, screens, and the downspout for all conditions tested. Thus, it was decided to test both a preblend of colloidal silicon dioxide with the API in addition to testing each of these components individually. Since the silicon dioxide is a minor component, the feeding range for these trials is similar to the API feeding trials, meaning that the same feeder and tooling combinations should be investigated. It was unknown whether the preblended API and silica would adhere to the flights of the coarse auger screws, so these were also tested for compatibility and performance.

4.5 Magnesium Stearate

Magnesium stearate is used in small amounts as a lubricant to enable release of the compacted tablets from the tooling of a tablet press. This powder is easily sheared, and also tends to coat other powders and metal surfaces. Both of these properties contribute to giving MgSt its lubricant functionality. However, these properties also make MgSt a challenging material to handle, as it tends to coat metal tooling and tends to be shear sensitive. The desired flowrate range for magnesium stearate was 0.177 to 0.2777 kg/hr (1.3 to 2 dm^3/hr), which is in the middle to upper range for the capacity of the K-Tron MT12. As initial testing with magnesium stearate showed it had a tendency to coat the metal tooling, it was tested only with the "self-cleaning" screws: coarse concave screws (CCS) and fine concave screws (FCS). Five screen conditions were available to be paired with both of these screws: coarse square screen (CSqS), fine square screen (FSqS), coarse slotted screen (CSlS), fine slotted screen (FSlS), and no screen (NoS).

Since manual refilling of the K-Tron MT12 may be difficult due to the need to refill it relatively often, testing was also carried out using the K-Tron KT20 feeder, which has a much larger hopper. This feeder was only tested for the fine concave screws (FCS), because the coating issue required self-cleaning screws and the low feedrate required fine screws. Once again, all four screen conditions were tested.

4.6 Crospovidone

Crospovidone is used in small amounts in tablet formulations as a disintegrant. The desired flowrate range for crospovidone, 0.480 to 0.750 kg/hr (1.5 to 2.2 dm^3/hr), falls on the upper range of the MT12 and on the lower end of the KT20. Initial testing in the K-Tron MT12 revealed that the upper end of the range could not be achieved consistently, so testing was limited to the KT20. The reason the MT12 was unable to achieve the upper end of the desired feedrate setpoint may have been due to fluctuations in density or flight filling. Self-cleaning screws were needed in order to remove the potential material buildup on the screws. This left a single pair of screws to be tested in the KT20, the fine concave screws (FCS). These screws were paired with all four screen condition options: coarse square screen (CSqS), medium square screen (MSqS), fine square screen (FSqS), and no screen (NoS).

5 Results

5.1 ProSolv HD90

Acceptable performance was achievable in both tested feeders: KT35 and KT20. The feeding performance is shown in Figure 6. In the KT35, performance is quickly divided into two sets of observations with very different performance values. In the poorly

performing set, characterized by higher RSD values, the oscillations are due to the powder flowing too freely with respect to the tooling. This causes pulsations as the screws turn, due to the powder emptying or flushing out of each flight of the screws with each rotation. This situation is greatly improved by using the concave screws that have smaller pockets, and thus smaller pulsations. Discharge screens also contributed to performance improvement by holding the powder in the screw flights and not allowing it to flush out freely.

As the desired throughput of the Prosolv HD90 fell on the lower end of the KT35, performance was also examined in the smaller KT20 feeder. Performance of the two feeders (KT35 and KT20) is compared in Figure 7a,b,, suggesting that the KT20, in general, is a better fit for the throughput, but comparable performance can be achieved with the KT35 with the proper tooling selections. In the KT20, it was found that the best configuration was the coarse concave "self-cleaning" screws (CCS) with the coarse square screen (CSqS).

To determine the actual magnitude of feedrate variations, not just their relative impact, the feedrate data can be plotted with respect to time and can be compared to variations observed for multiple feeder and tooling combinations. Figure 8 a, b, c show the feedrate as a function of time for several configurations. To demonstrate the importance of the sampling interval and the impact of averaging, each of these figures show the actual sampled feedrate data (sampling time of 0.1 seconds) as well as moving averages for several time intervals. Figure 8a shows a poorly performing condition in the KT35 using the fine auger screw. This results in very large oscillations. In Figure 8b, the magnitude of the oscillations is decreased using the fine concave screws, but the frequency is

similar. Figure 8c, which shows data obtained using the smaller KT20, demonstrates that the magnitude of deviations is further reduced, but in addition the frequency of oscillations is increased. This represents a significant improvement, since higher frequency oscillations will be more effectively filtered by axial mixing in the blenders and other processing units downstream of the feeders.[28]

Figure 10 further highlights the importance of the sampling interval when reporting relative standard deviation of a feedrate. Figure 10a is a rescaled version of the plot shown in Figure 8a, which is the feeding data from the K-Tron KT35 feeding ProSolv without a screen. This condition leads to very large, almost sinusoidal oscillations. In this figure, moving averages are plotted for 0.1s intervals, which is the sampling interval of the data collection. If the sampling frequency is reduced, the sampling interval would be larger and result in data points like those shown in Figure 10b. For the sampling intervals larger than 1 second, there is an inability to detect the actual oscillatory nature of the feedrate.

When the sampling or moving average interval is increased, the relative standard deviation quickly decreases as shown in Figure 10c. A common but misleading practice that is often used by feeding equipment manufacturers is to use a relative standard deviation for a 60s interval, which results almost always in very low levels for RSD. Considering that the next unit operation for this manufacturing process is a continuous blender that may have a residence time shorter than 60s, using a sampling interval this long is both conceptually wrong and potentially misleading. A sampling interval should be short enough to detect fluctuations that are pertinent to the process, which means that

sampling needs to be much faster than the residence time of the subsequent unit operations.

Figure 9 shows the performance data for the KT20 for each screen condition: no screen (NoS), coarse square screen (CSqS), medium square screen (MSqS), and fine square screen (FSqS). For each condition, it is shown that the two screws perform in similar manner. Main differences are observed only with the use with the coarse square screen at all feedrate setpoints, and when using no screen for high speeds. The data suggests that the coarse concave screw performs slightly better, but as the screens become finer the effect from the screw type becomes less important. As a whole, these differences in performance shown in the KT20 can be considered minor.

5.2 Active Pharmaceutical Ingredient (API)

Figure 11 shows the feeding performance results from the feeding the API powder in the K-Tron KT20. For some of the screens, testing with this material resulted in autoshutdown alarms in the feeder, which is meant to prevent damage to the equipment. The cause of this run time failure was that the openings in the screen were too small for the rates that were needed and so the powder could not pass through the screen fast enough, resulting in clogging and ultimately compaction of the powder in the discharge tube. This raised the torque needed to rotate the screws, which is how the feeder detected the problem. The screens incompatible with the API were the medium square screen (MSqS) and the fine square screen (FSqS). See Table 14.

Due to the incompatibilities that were shown with some of the screens, it was concluded that API would be best fed without discharge screens, thereby avoiding the potential for

feeder alarm from the clogging of the screens. While the feedrates could potentially be fed in the K-Tron KT35, larger screws often require discharge screens. After observation of the compatibility problems with the discharge screens in the K-Tron KT20, feeding in the KT35 with discharge screens was determined to be non-viable.

5.3 Colloidal Silicon Dioxide (Silica)

Colloidal Silicon Dioxide was anticipated to pose the largest feeding challenges. As mentioned, this material is very low density and has intense electrostatic properties, which causes it to display a strong tendency to adhere to the downspout on the outlet of the feeder. Thus, the plan was to test this material with the largest array of tooling options, but tooling compatibility quickly reduced the available options. Moreover, in an attempt to suppress the effect of electrostatics, the discharge of the feeder was instrumented with a static eliminator. The static eliminator consisted of an ion generator and a small air flow, which could contribute to eliminate static charge development and reduce the tendency of the material to adhere to the feeder. Figure 12a shows the buildup of material that occurred without the static eliminator and Figure 12b shows the assembly of the static eliminator attached to the outlet of the feeder. In Figure 13a,b, the effect of the static eliminator was examined. It is shown that there is more material adhering to the feeder without the static eliminator. However, while the problem was reduced, it was not eliminated; even when a static eliminator was used, there was still significant material buildup. This was considered unacceptable, as the material sticking at the feeder discharge would eventually fall into the mixer, intermittently raising the concentration of silica in the formulation, resulting in product containing higher silicon dioxide content than the formulation specification.

In Figure 14, the feeding performance of the silicon dioxide in both the KT20 and KT35 is shown. The effect of using the static eliminator is also shown. Use of the static eliminator showed an improvement in feeding performance. In addition, the more consistent flight filling of the larger screws in the KT35 also caused improvements in the feeding performance as compared to the smaller screws of the KT20. Use of a metal surface coating, Impreglon, also showed a significant improvement. Based on performance alone, it was possible to feed the material and minimize variability. However, it must also be considered that during the short runtime of the experimental feeding trials, material that built up on the feeder did not fall out of the downspout. In longer runs used for commercial manufacturing, this would indeed happen, causing spikes in the silica feedrate. Thus the feeding performance observed in Figure 14 may not be representative of what would be observed in a long-running process. As such, it was concluded that silica should not be fed as a pure component, and that instead it should be either eliminated from the formulation or preblended with another ingredient, such as the API.

5.4 API and Silica Preblend

Figure 15 shows the feeding performance results from the feeding of the API and silica preblend in the K-Tron KT20. Similar to the pure API trials, tests utilizing the fine square screen (FSqS) resulted in autoshutdown alarms in the feeder. See Table 15. Differing from the API, the preblend was compatible with the medium square screen (MSqS), which is due to the addition of the colloidal silicon dioxide that improved flow.

Due to the incompatibilities that were shown with some of the screens, it was concluded that API / silica preblend would be best fed without discharge screens, thereby avoiding

the potential motor overload alarm caused by the clogging of the screens. The performance between screws without screens was concluded to be similar, although the coarse concave screws are preferred as they eliminate the potential for material buildup within the flights of the screws, even though no material buildup was observed during these trials.

5.5 Magnesium Stearate

As mentioned, Magnesium stearate is a lubricant known to have a tendency to coat and smear on metal parts. As such, it was decided that all the testing for this powder would be carried out with concave self-cleaning screws. The feeding performance of MgSt for the MT12 is displayed in Figure 16. In general, the tooling did not play a large role in the feeding performance of MgSt. The fine concave screw performed the best. There was not a significant improvement from the usage of screens, so it was concluded that the best performance would be obtained without a screen.

When testing in the larger KT20 feeder, it was noticed that the control magnitude of the feeder drifted. It was also noticed that the feeding performance changed as a function of time, as seen in Figure 17. In the figure, the order of the runs was, first, without screen (NoS), then another shorter run without screen, then a run using the coarse square screen (CSqS), the medium square screen (MSqS), and the fine square screen (FSqS). Subsequently, the run without the screen was repeated. After each run, it was noticed that the drive command decreased from start to finish. This time-dependent behavior is most likely caused by the long residence time of the powder in the hopper. As the hopper size is much larger for the KT20, this leads to repetitive shearing due to the hopper agitation.

This led to the investigation of long runs with this powder in order to determine long term performance, which is shown in Figure 18 in both feeders. With the KT20, the feeder performance became worse over time, which can be shown by the increasing RSD. For the MT12, there was a slight increase in RSD, but it was not nearly as large as shown by the resulting horizontal plot for the MT12 in Figure 18. The sudden dips in RSD shown for the MT12 correspond to the hopper refills which occurred at ~70 minutes and ~120 minutes, indicating that it is a change in powder behavior.

The difference between the KT20 and MT12 in the drifting behavior of the RSD for magnesium stearate may be due to a residence time difference (as the KT20 is much longer), but it may also be due to design differences affecting how the hoppers are agitated. The KT20 uses a horizontal axis with an over-under rotation, located at the bottom of the powder bed, which may lead to very intense shear. Due to the smaller size, the MT12 has much less powder, but also uses an agitator that rotates along the vertical axis of the hopper, acting in a stirring motion resulting in less shearing against the downward weight of the entire bed.

When comparing the KT20 and MT12's long term performance, it is quite obvious that the MT12 performs better. The one main advantage to the KT20 is that it has a larger hopper and will not require refills as often which makes for a refill scheduling that is easier to maintain.

5.6 Crospovidone

Crospovidone is fed at a low rate in the KT20. Figure 19 shows the feeding performance from the KT20. This powder fed relatively easily with no significant problems being

observed in feeding performance. Using the RSD vs. feedrate plot, the best performing tooling combination can be easily determined. The lowest RSD across the desired feedrate range is displayed by the fine concave screws (FCS) and the medium square screen (MSqS).

5.7 Effects of feeding conditions on powder flow properties

Each powder was tested in the Freeman Tech FT4 powder rheometer before and after feeding in order to detect any changes in the powder caused by the feeding process. Two tests were used: compressibility and the shear cell test. An example of the compressibility test for Prosolv HD90 is shown in Figure 20. Compressibility is a bulk property that is measured in the FT4 by conditioning the powder followed by slowly compressing, while letting entrained air escape. Compressibility can indicate whether a powder is cohesive or free flowing [29]–[31]. The compressibility for this powder was found to be low (~7%) which indicates that it is a free flowing powder. Minor differences between the fed and unfed powder were observed, but the effect of tooling was not found to be statistically significant. All of the powders in the formulation had similar plots with the same conclusion that the effect of feeding on the discharged powder properties, if any, was independent of feeder tooling. This means that the selection of optimal feeder and tooling was independent of changes to the powder flow properties. However, since feeding does increase the compressibility of the pure components, this needs to be considered, when characterizing the rest of the downstream processes.

An example of the shear cell test results for the Prosolv HD90 is shown in Figure 21. As all of the plots also overlap, there is no significant difference due to the powder feeding process. This same result and conclusion also applied to the other powders in the

formulation. Significant changes in shear cell results would have been expected if the powders were extremely shear sensitive as the feeders do not heavily shear the materials.

6 Conclusions

This study was for a specific formulation, but the same methods used can be applied to other formulations. The process for tooling optimization can be described with the following list of steps:

1. Select potential feeders and tooling
2. Screen the tooling for compatibility issues
3. Test compatible conditions and monitor feedrate

Initial selection of the feeders to be tested was based on the theoretical volumetric throughput of the different tooling configurations for the feeders. The ability of a feeder to achieve these volumetric throughputs depends on the powder properties of the powder. If the powder does not flow easily in the flights of the screws, the flight fill fraction will be less than ideal and the theoretical throughput will be higher than actual throughput.

During gravimetric feeding trials, selection of the proper sampling interval is very important. An interval that is too long relative to the subsequent processing will not adequately detect fluctuations. When recording relative standard deviation the sampling time is needed for reference as relative standard deviations with differing sampling intervals cannot be compared fairly.

After potential feeders and tooling are selected, the testing should be narrowed to only compatible tooling. Tooling can be found to be incompatible for several reasons based on powder properties.

- Screws tend to fail due to material adhering within the flights or in the case of flight filling issues. If material is adhering within the screws, this will be observed after running the feeder with the selected screw when the feeder is disassembled and the screws are visible. If this problem observed, then self-cleaning concave screws should be used. In the presence of flight filling issues, the feeder will run at a higher RPM than the theoretical rate, which may not be a problem unless the feeder is running at the top screw speed. In extreme cases, which were not observed in the tested formulation, powder bridging in the hopper leads to "rat holing" or tunneling. Such cases may lead eventually to no powder entering the flights of the screws. Larger screws or even larger flights tend to improve flight filling.
- Screens tend to fail with very cohesive and/or shear sensitive materials. With free flowing materials, screens create an extra barrier that prevents material from flooding out of the feeder. With cohesive materials they serve to break up clumps of material into a more smooth flowing stream. Because they still act as a barrier even with cohesive materials or shear sensitive materials, they increase the overall shear on the material and also the holes in the screen may clog with cohesive material. An additional failure occurs for materials that tend to adhere to surfaces, as this adds another surface that material can deposit.

There are other non-tooling dependent problems that could potentially affect the long term performance of a continuous process. Significantly, it is important to minimize the amount of material that adheres to surfaces. For the case study discussed here, these effects are most critical for the colloidal silicon dioxide. This is a common ingredient

used in many formulations. Feeding of this powder as a pure component proved to be very unreliable. Thus, it is recommended that the colloidal silicon dioxide be preblended with another ingredient that is thus used as a carrier. In most formulations, the best choice of this carrier is likely to be the API, since the usual purpose of adding silicon dioxide, a glidant, is to improve API flow properties. For the process of interest here, preblending of silica would enable the process to be carried out using 4 feeders dispensing each material into the blender: API / silica preblend, Prosolv HD90, Magnesium Stearate, and Crosspovidone.

7 References

[1] K. Plumb, “Continuous Processing in the Pharmaceutical Industry: Changing the Mind Set,” *Chem. Eng. Res. Des.*, vol. 83, no. 6, pp. 730–738, Jun. 2005.

[2] FDA, “Guidance for Industry: PAT - a framework for innovative pharmaceutical development, manufacturing and quality assurance.” Food and Drug Administration, 2004.

[3] K. R. Wilburn, “The business case for continuous manufacturing of pharmaceuticals,” Thesis, Massachusetts Institute of Technology, 2010.

[4] H. Leuenberger, “New trends in the production of pharmaceutical granules: batch versus continuous processing,” *Eur. J. Pharm. Biopharm.*, vol. 52, no. 3, pp. 289–296, Nov. 2001.

[5] G. Betz, P. Junker-Bürgin, and H. Leuenberger, “Batch And Continuous Processing In The Production Of Pharmaceutical Granules#,” *Pharm. Dev. Technol.*, vol. 8, no. 3, pp. 289–297, 2003.

[6] S. Buchholz, “Future manufacturing approaches in the chemical and pharmaceutical industry,” *Chem. Eng. Process. Process Intensif.*, vol. 49, no. 10, pp. 993–995, Oct. 2010.

[7] S. D. Schaber, D. I. Gerogiorgis, R. Ramachandran, J. M. B. Evans, P. I. Barton, and B. L. Trout, “Economic Analysis of Integrated Continuous and Batch Pharmaceutical Manufacturing: A Case Study,” *Ind. Eng. Chem. Res.*, vol. 50, no. 17, pp. 10083–10092, Sep. 2011.

[8] R. Singh, F. Boukouvala, E. Jayjock, R. Ramachandran, M. Ierapetritou, and F. Muzzio, “Flexible multipurpose continuous processing of pharmaceutical tablet manufacturing process,” *GMP News Eur. Compliance Acad. ECE*, 2012.

[9] R. Singh, M. Ierapetritou, and R. Ramachandran, “An engineering study on the enhanced control and operation of continuous manufacturing of pharmaceutical tablets via roller compaction,” *Int. J. Pharm.*, vol. 438, no. 1–2, pp. 307–326, Nov. 2012.

[10] R. Singh, M. Ierapetritou, and R. Ramachandran, “System-wide hybrid MPC–PID control of a continuous pharmaceutical tablet manufacturing process via direct compaction,” *Eur. J. Pharm. Biopharm.*

[11] R. Singh, M. Ierapetritou, and R. Ramachandran, “Hybrid advanced control of flexible multipurpose continuous tablet manufacturing process via direct compaction,” in *Computer Aided Chemical Engineering*, vol. Volume 32, Andrzej Kraslawski and Ilkka Turunen, Ed. Elsevier, 2013, pp. 757–762.

[12] R. Weinekotter and L. Reh, “Continuous Mixing of Fine Particles,” *Part. Part. Syst. Charact.*, vol. 12, no. 1, pp. 46–53, 1995.

[13] P. V. Danckwerts, “Continuous flow systems: Distribution of residence times,” *Chem. Eng. Sci.*, vol. 2, no. 1, pp. 1–13, Feb. 1953.

[14] J. C. Williams and M. A. Rahman, “Prediction of the performance of continuous mixers for particulate solids using residence time distributions: Part II. Experimental,” *Powder Technol.*, vol. 5, no. 5, pp. 307–316, Apr. 1972.

[15] L. Pernenkil and C. L. Cooney, “A review on the continuous blending of powders,” *Chem. Eng. Sci.*, vol. 61, no. 2, pp. 720–742, Jan. 2006.

[16] R. Singh, F. Boukouvala, E. Jayjock, R. Ramachandran, M. Ierapetritou, and F. Muzzio, “Flexible multipurpose continuous processing,” *Pharm Process*, vol. 27, no. 6, pp. 22–25, 2012.

[17] J. Dai, H. Cui, and J. R. Grace, “Biomass feeding for thermochemical reactors,” *Prog. Energy Combust. Sci.*, vol. 38, no. 5, pp. 716–736, Oct. 2012.

[18] S. Yang and J. R. G. Evans, “Metering and dispensing of powder; the quest for new solid freeforming techniques,” *Powder Technol.*, vol. 178, no. 1, pp. 56–72, Sep. 2007.
[19] J. Dai and J. R. Grace, “A model for biomass screw feeding,” *Powder Technol.*, vol. 186, no. 1, pp. 40–55, Aug. 2008.
[20] J. B. Myhre and S. Ludescher, “Apparatus and method for controlling flow rate in vibratory feeders,” 5341307, 23-Aug-1994.
[21] J. C. Homer, III, J. R. Walsh, and D. P. Ratcliffe, “System for checking the calibration of gravimetric feeders and belt scales ...,” 5686653, 11-Nov-1997.
[22] N. Somsuk, T. Wessapan, and S. Teekasap, “Design and Development of a Rotary Airlock Valve for Using in Continuous Pyrolysis Process to Improve Performance,” *Adv. Mater. Res.*, vol. 383–390, pp. 7148–7154, Nov. 2011.
[23] K-Tron, “K-Tron Operating Instruction: KSU-II/KCM-KD Operation for LWF, WBF, PID, SFM and VOL Applications.” Pitman, NJ: K-Tron, 2006.
[24] M. Hopkins, “LOSS in weight feeder systems,” *Meas. Control*, vol. 39, no. 8, pp. 237–240, 2006.
[25] V. Kehlenbeck and K. Sommer, “Possibilities to improve the short-term dosing constancy of volumetric feeders,” *Powder Technol.*, vol. 138, no. 1, pp. 51–56, Nov. 2003.
[26] G. Tardos and Q. Lu, “Precision dosing of powders by vibratory and screw feeders: an experimental study,” *Adv. Powder Technol.*, vol. 7, no. 1, pp. 51–58, 1996.
[27] W. E. Engisch and F. J. Muzzio, “Method for characterization of loss-in-weight feeder equipment,” *Powder Technol.*, vol. 228, no. 0, pp. 395–403, Sep. 2012.
[28] Y. Gao, F. Muzzio, and M. Ierapetritou, “Characterization of feeder effects on continuous solid mixing using fourier series analysis,” *AIChE J.*, vol. 57, no. 5, pp. 1144–1153, 2011.
[29] R. Freeman and X. Fu, “Characterisation of powder bulk, dynamic flow and shear properties in relation to die filling,” *Powder Metall.*, vol. 51, no. 3, pp. 196–201, 2008.
[30] R. Freeman, “Measuring the flow properties of consolidated, conditioned and aerated powders — A comparative study using a powder rheometer and a rotational shear cell,” *Powder Technol.*, vol. 174, no. 1–2, pp. 25–33, May 2007.
[31] A. Vasilenko, B. J. Glasser, and F. J. Muzzio, “Shear and flow behavior of pharmaceutical blends — Method comparison study,” *Powder Technol.*, vol. 208, no. 3, pp. 628–636, Apr. 2011.

8 Figures

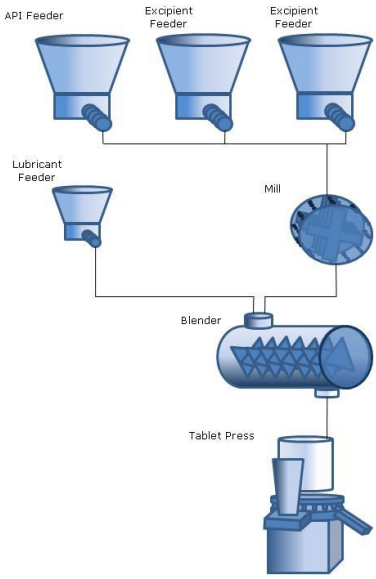

Figure 1: Diagram of a direct compression continuous process

Figure 2: K-Tron KT35 feeder with Schenck Accurate AccPro II catch scale, K-Tron KT20 feeder, and K-Tron MT12 feeder.

The final publication is available at Springer via http://dx.doi.org/10.1007/s12247-014-9206-1

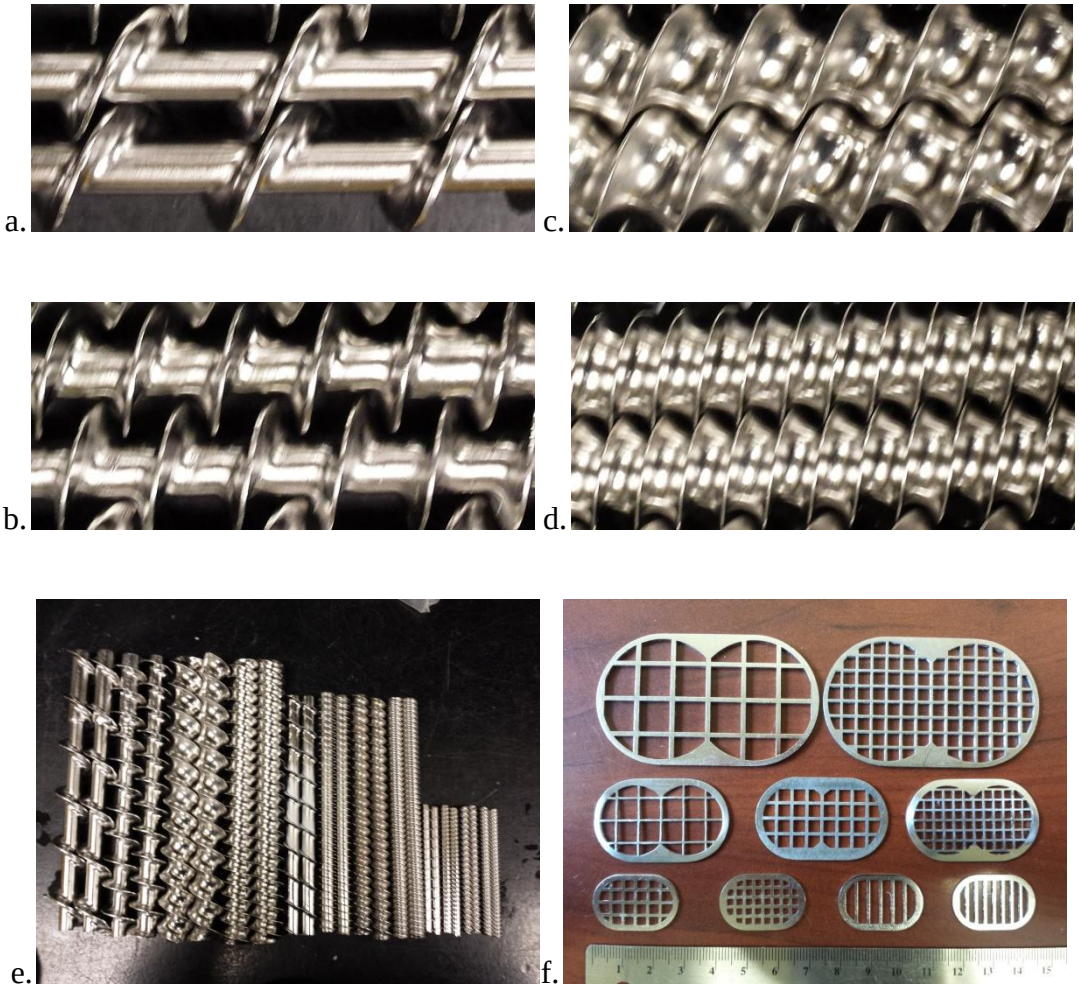

Figure 3: K-Tron twin-screw feeder tooling. Each feeders tooling consists of 4 sets of twin screws: a) coarse auger screw (CAS), b) fine auger screw (FAS), c) coarse concave screw (CCS), and d) fine concave screw (FCS). e) The screws from each feeder are only compatible with that feeder as they are different sizes. f) The screens for all the feeders are displayed together for comparison. KT35 has two screens (top): fine square screen (FSqS) and coarse square screen (CSqS). The KT20 has three screens (middle): fine square screen (FSqS), medium square screen (MSqS), and coarse square screen (CSqS). The MT12 has four screens (bottom): fine square screen (FSqS), coarse square screen (CSqS), fine slotted screen (FSlS), and coarse slotted screen (CSlS). All of the feeders can also be run without a screen (NoS)

a.

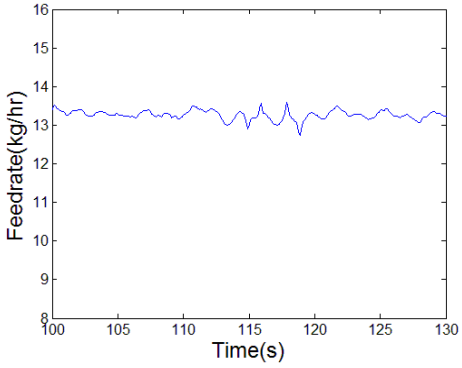

b.

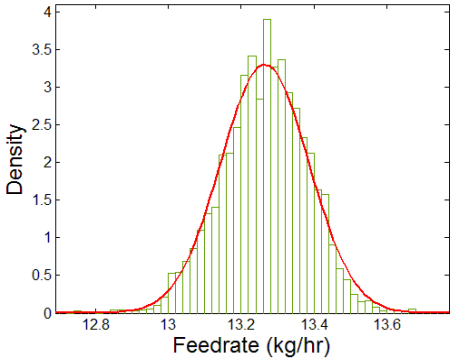

Figure 4: a) Time series data and b) probability distribution function (PDF) for the KT20 with Coarse Concave Screws (CCS) and Medium Square Screen (MSqS) feeding Prosolv at 13.3 kg/hr.

The final publication is available at Springer via http://dx.doi.org/10.1007/s12247-014-9206-1

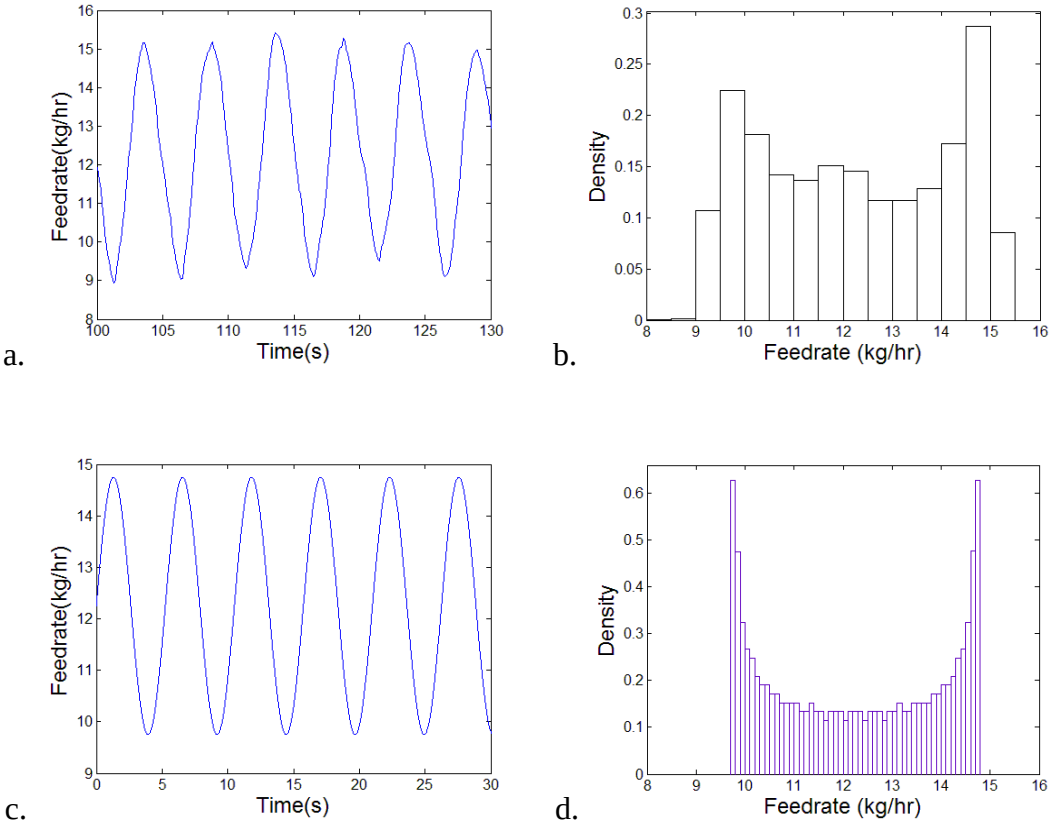

Figure 5: a) Time series data and b) probability distribution function (PDF) for the KT35 with Fine Auger Screws (FAS) and No Screen (NoS) feeding Prosolv at 13.3 kg/hr. For comparison, c) Simulated Sine wave and d) its PDF.

The final publication is available at Springer via http://dx.doi.org/10.1007/s12247-014-9206-1

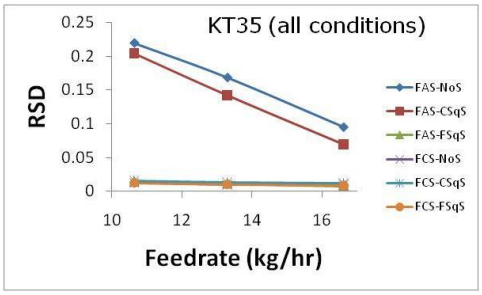

Figure 6: Feeding performance as RSD as a function of feedrate for the KT35 feeding Prosolv HD90. See Figure 7a for a rescaled plot showing the best conditions.

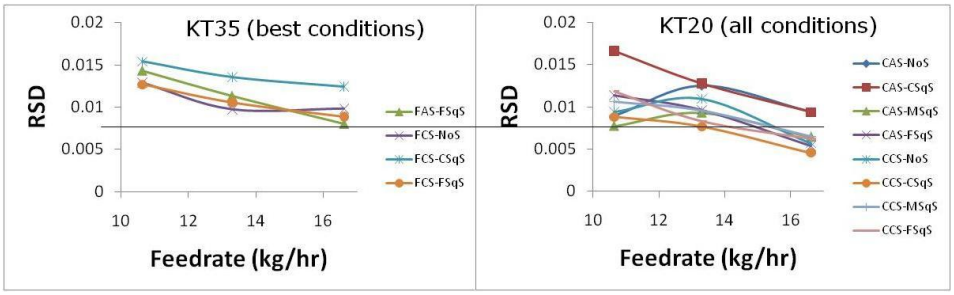

Figure 7: Feeding performance of Prosolv HD90 being fed by (a) KT35 and (b) KT20

The final publication is available at Springer via http://dx.doi.org/10.1007/s12247-014-9206-1

a.

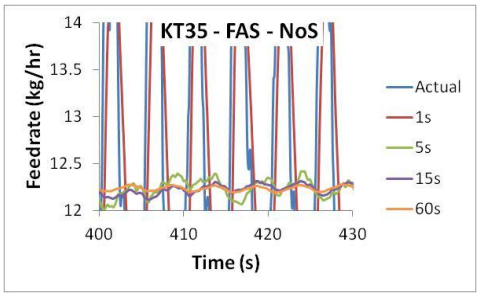

b.

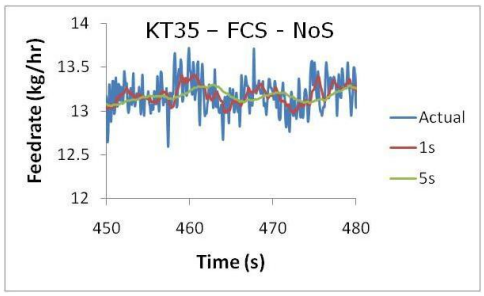

c.

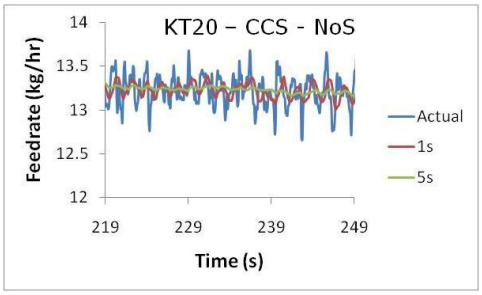

Figure 8: Feedrate data as a function of time for the feeding of Prosolv HD90 being fed from (a) KT35 with fine auger screws and no screen, (b) KT35 with fine concave screws and no screen, and (c) KT20 with coarse concave screws and no screen.

The final publication is available at Springer via http://dx.doi.org/10.1007/s12247-014-9206-1

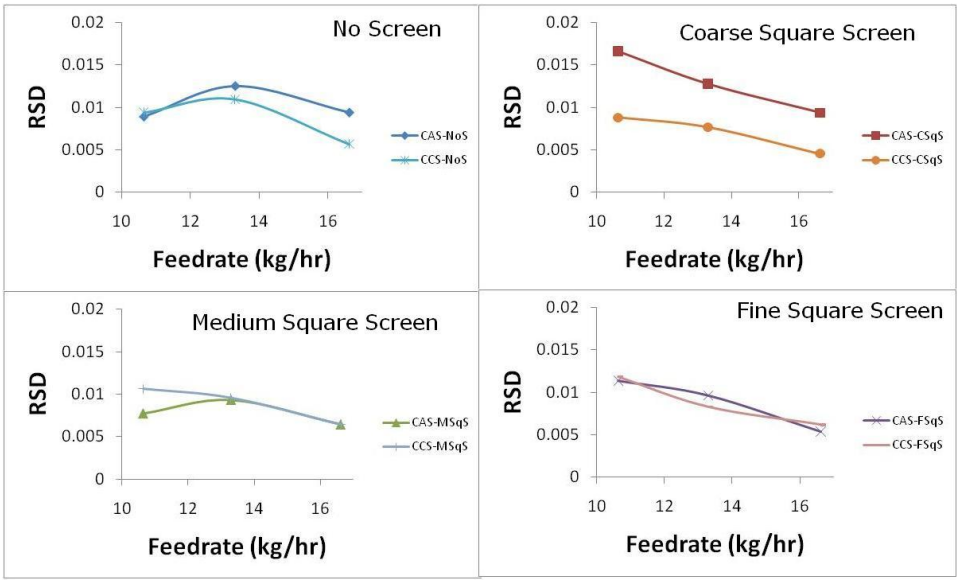

Figure 9: Feeding performance of KT20 feeding Prosolv HD90.

The final publication is available at Springer via http://dx.doi.org/10.1007/s12247-014-9206-1

a.

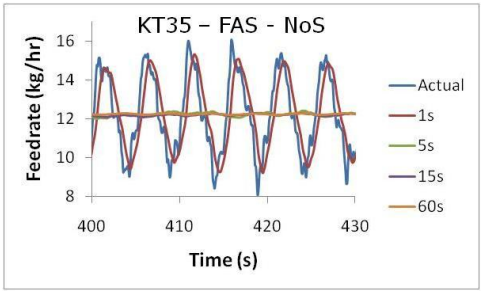

b.

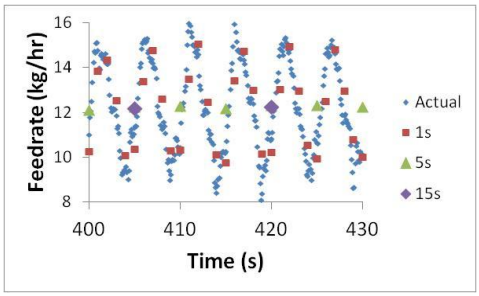

c.

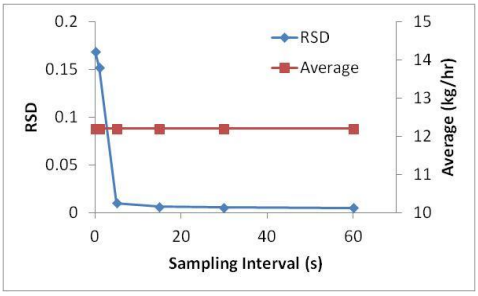

Figure 10: Feedrate data as a function of time for the feeding of Prosolv HD90 being fed from KT35 with fine auger screws and no screen displayed (a) using different moving averages and (b) using simulated sampling intervals. (c) The effect of sampling interval on relative standard deviation (RSD).

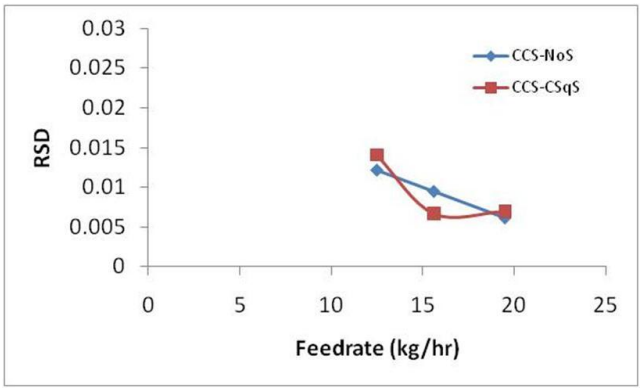

Figure 11: Feeding performance of pure component API fed by the K-Tron KT20

Figure 12: Picture of feeder (a) without static eliminator and (b) with static eliminator

Figure 13: Picture of silicon dioxide buildup for (a) without static eliminator and (b) with static eliminator

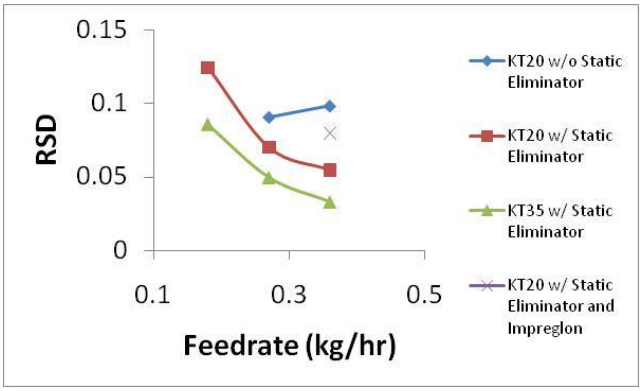

Figure 14: Feeding performance of both KT35 and KT20 feeders feeding silicon dioxide

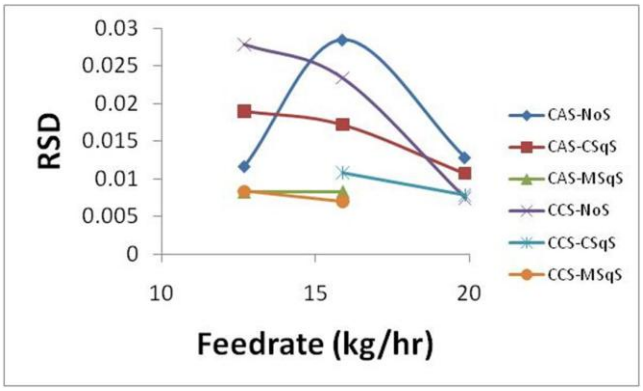

Figure 15: Feeding performance of API / Silica blend fed by the K-Tron KT20

The final publication is available at Springer via http://dx.doi.org/10.1007/s12247-014-9206-1

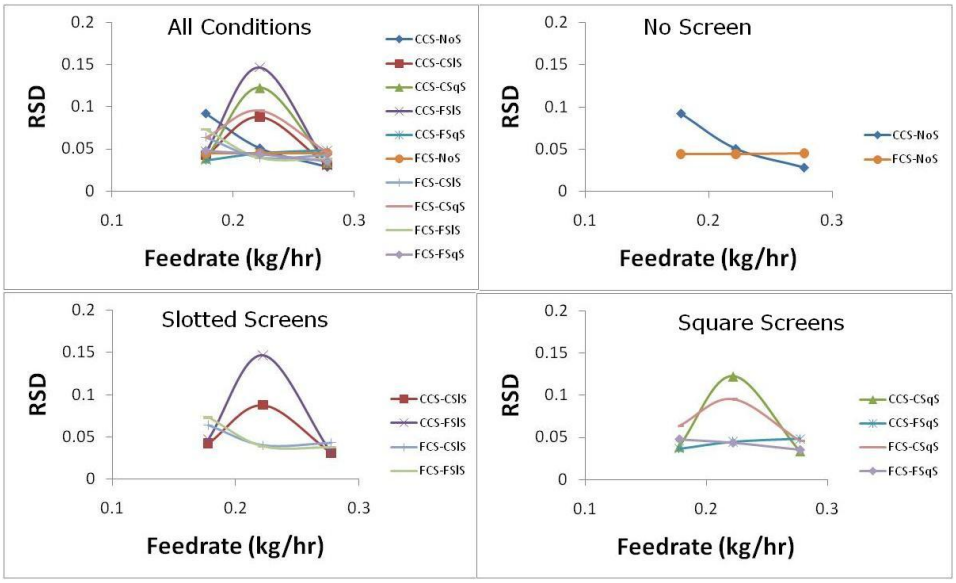

Figure 16: Feeding performance of MT12 feeding magnesium stearate

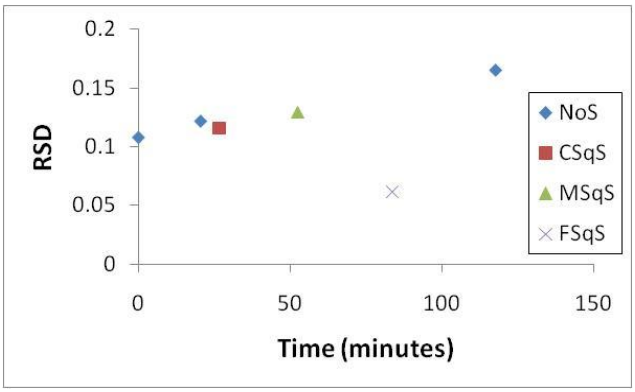

Figure 17: Feeding performance of KT20 feeding magnesium stearate at nominal feedrate

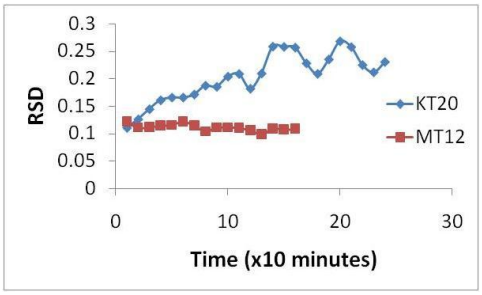

Figure 18: Long term feeding performance for the feeding of magnesium stearate being fed by KT20 and MT12

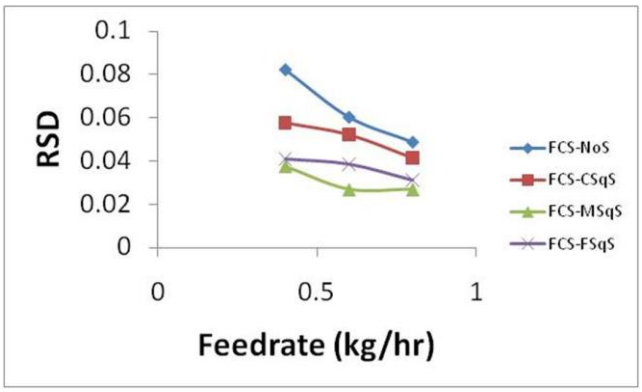

Figure 19: Feeding performance for the KT20 feeding crospovidone

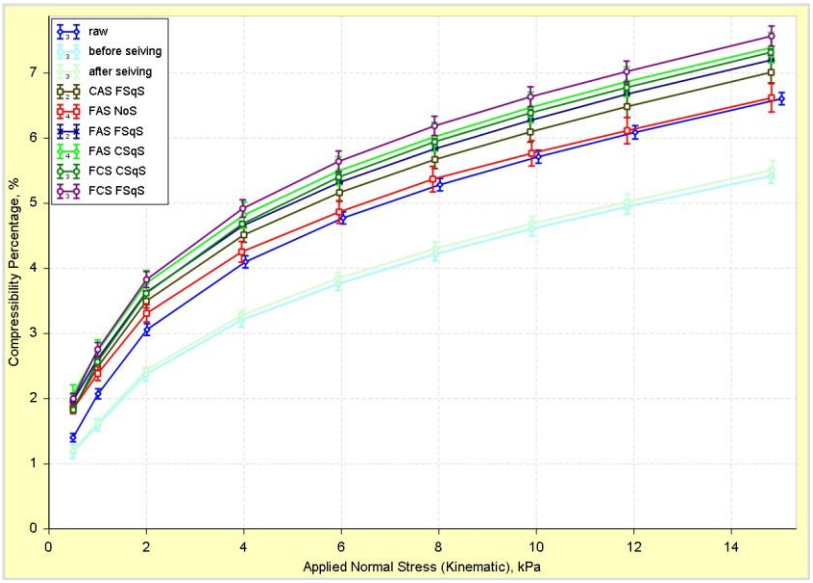

Figure 20: Freeman Tech FT4 compressibility results for Prosolv HD90 being fed with various feeder tooling. No significant effect of feeder configuration was found.

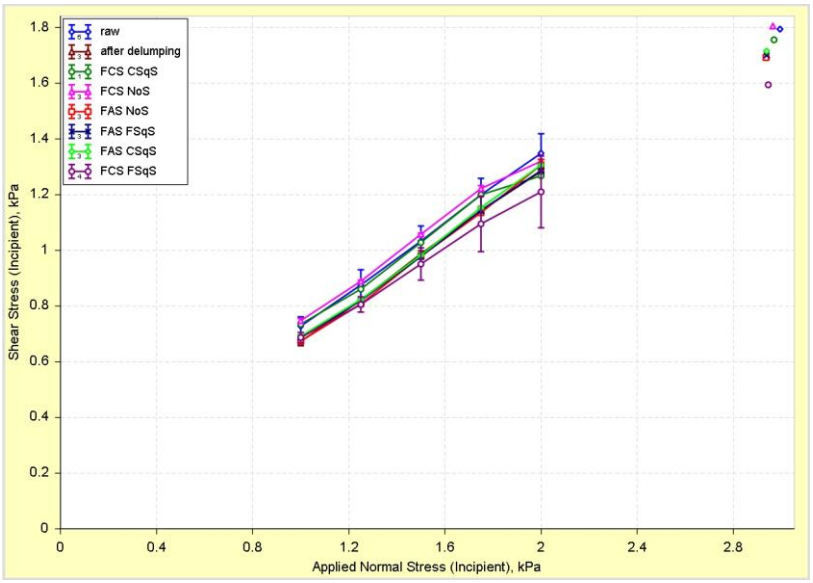

Figure 21: Freeman Tech FT4 shear cell test results for Prosolv HD90 being fed with various feeder tooling. No significant effect of feeder configuration was found.

9 Tables

Table 1: Feeder capacity of K-Tron feeders

Model	Volumetric Throughput (dm^3/hr)		Gravimetric Throughput (kg/hr)*		Hopper Capacity	
	Low	High	Low	High	dm^3	kg*
K-Tron KT35	1.8	2500	0.9	1250	25	12.5
K-Tron KT20	0.1	200	0.05	100	25	12.5
K-Tron MT12	0.04	4	0.02	2	2	1

*Gravimetric Throughput assumes a bulk density of 0.5 kg/dm^3.

Table 2: List of available screens for each K-Tron feeder model

Feeder	CSqS	MSqS	FSqS	CSlS	FSlS	NoS
KT35	X		X			X
KT20	X	X	X			X
MT12	X		X	X	X	X

Table 3: Formulation

Component	Manufacturer	Function	% w/w
API		Active	52.02
Prosolv HD90	JRS Pharma	Filler	44.33
Colloidal Silicon Dioxide (Cab-O-Sil M5P)	Cabot	Glidant	0.91
Crospovidone (Polyplasdone XL-10)	ISP	Disintigrant	2
Magnesium Stearate (Grade 5712)	Mallinckrodt	Lubricant	0.74
		Total	100

Table 4: Component gravimetric and calculated volumetric feedrates

Component	API	Prosolv HD90	Colloidal Silicon Dioxide	Crospovidone	Magnesium Stearate
% w/w	52.02	44.33	0.91	2	0.74
Nominal Feedrate (kg/hr)	15.606	13.299	0.273	0.6	0.222
80%	12.485	10.639	0.2184	0.4800	0.1776
100%	15.606	13.299	0.2730	0.6000	0.2220
125%	19.508	16.624	0.3413	0.7500	0.2775
Density (kg/dm3)	0.61	0.49	0.04	0.33	0.14
Volumetric Rates (dm3/hr)					
80%	20.47	21.71	5.46	1.45	1.27
100%	25.58	27.14	6.83	1.82	1.59
125%	31.98	33.93	8.53	2.27	1.98

Table 5: Volumetric Capacity for the K-Tron KT35

	Volumetric Feedrate (dm^3/hr)		RPM	
Screw	MIN	MAX	MIN	MAX
Coarse Concave Screw (CCS)	62	849	24	327
Coarse Auger Screw (CAS)	64	882	24	327
Fine Concave Screw (FCS)	21	294	24	327
Fine Auger Screw (FAS)	23	310	24	327

Table 6: Volumetric Capacity for the K-Tron KT20

	Volumetric Feedrate (dm^3/hr)		RPM	
Screw	MIN	MAX	MIN	MAX
Coarse Concave Screw (CCS)	2.5	34	12	170
Coarse Auger Screw (CAS)	2.7	37	12	170
Fine Concave Screw (FCS)	0.93	13	12	170
Fine Auger Screw (FAS)	1	14	12	170

Table 7: Volumetric capacity of the K-Tron MT12

Screw	Volumetric Feedrate (dm^3/hr)		RPM	
	MIN	MAX	MIN	MAX
Coarse Concave Screw (CCS)	0.1	4	0.5	100
Coarse Auger Screw (CAS)	0.1	4	0.5	100
Fine Concave Screw (FCS)	0.04	2.2	0.5	100
Fine Auger Screw (FAS)	0.04	2.2	0.5	100

Table 8: Feeder testing configurations for Prosolv HD90

KT20		Prosolv HD90 80%	100%	125%
CCS	CSqS	X	X	X
	MSqS	X	X	X
	FSqS	X	X	X
	NoS	X	X	X
CAS	CSqS	X	X	X
	MSqS	X	X	X
	FSqS	X	X	X
	NoS	X	X	X
FCS	CSqS			
	MSqS			
	FSqS			
	NoS			
FAS	CSqS			
	MSqS			
	FSqS			
	NoS			

KT35		Prosolv HD90 80%	100%	125%
CCS	CSqS			
	FSqS			
	NoS			
CAS	CSqS			
	FSqS			
	NoS			
FCS	CSqS	X	X	X
	FSqS	X	X	X
	NoS	X	X	X
FAS	CSqS	X	X	X
	FSqS	X	X	X
	NoS	X	X	X

Table 9: Feeder testing configurations for API

KT20		API 80%	100%	125%
CCS	CSqS	X	X	X
	MSqS	X	X	X
	FSqS	X	X	X
	NoS	X	X	X
CAS	CSqS			
	MSqS			
	FSqS			
	NoS			
FCS	CSqS			
	MSqS			
	FSqS			
	NoS			
FAS	CSqS			
	MSqS			
	FSqS			
	NoS			

Table 10: Feeder testing configurations for colloidal silicon dioxide

KT20		Colloidal Silicon Dioxide 80%	100%	125%
CCS	CSqS			
	MSqS			
	FSqS			
	NoS	X	X	X
CAS	CSqS			
	MSqS			
	FSqS			
	NoS			
FCS	CSqS			
	MSqS			
	FSqS			
	NoS			
FAS	CSqS			
	MSqS			
	FSqS			
	NoS			

KT35		Colloidal Silicon Dioxide 80%	100%	125%
CCS	CSqS			
	FSqS			
	NoS	X	X	X
CAS	CSqS			
	FSqS			
	NoS			
FCS	CSqS			
	FSqS			
	NoS			
FAS	CSqS			
	FSqS			
	NoS			

Table 11: Feeder testing configurations for API and silicon dioxide preblend

KT20		API & Silica Blend 80%	100%	125%
CCS	CSqS	X	X	X
	MSqS	X	X	X
	FSqS	X	X	X
	NoS	X	X	X
CAS	CSqS	X	X	X
	MSqS	X	X	X
	FSqS	X	X	X
	NoS	X	X	X
FCS	CSqS			
	MSqS			
	FSqS			
	NoS			
FAS	CSqS			
	MSqS			
	FSqS			
	NoS			

Table 12: Feeder testing configurations for magnesium stearate

MT12		Magnesium Stearate 80%	100%	125%
CCS	CSqS	X	X	X
	FSqS	X	X	X
	CSIS	X	X	X
	FSIS	X	X	X
	NoS	X	X	X
CAS	CSqS			
	FSqS			
	CSIS			
	FSIS			
	NoS			
FCS	CSqS	X	X	X
	FSqS	X	X	X
	CSIS	X	X	X
	FSIS	X	X	X
	NoS	X	X	X
FAS	CSqS			
	FSqS			
	CSIS			
	FSIS			
	NoS			

KT20		Magnesium Stearate 80%	100%	125%
CCS	CSqS			
	MSqS			
	FSqS			
	NoS			
CAS	CSqS			
	MSqS			
	FSqS			
	NoS			
FCS	CSqS	X	X	X
	MSqS	X	X	X
	FSqS	X	X	X
	NoS	X	X	X
FAS	CSqS			
	MSqS			
	FSqS			
	NoS			

Table 13: Feeder testing configurations for crospovidone

KT20		Crospovidone 80%	100%	125%
CCS	CSqS			
	MSqS			
	FSqS			
	NoS			
CAS	CSqS			
	MSqS			
	FSqS			
	NoS			
FCS	CSqS	X	X	X
	MSqS	X	X	X
	FSqS	X	X	X
	NoS	X	X	X
FAS	CSqS			
	MSqS			
	FSqS			
	NoS			

Table 14: Changes to the API feeding trials. Tests marked with "InC" were found to be incompatible

KT20		API		
		80%	100%	125%
CCS	CSqS	X	X	X
	MSqS	InC	InC	InC
	FSqS	InC	InC	InC
	NoS	X	X	X
CAS	CSqS			
	MSqS			
	FSqS			
	NoS			
FCS	CSqS			
	MSqS			
	FSqS			
	NoS			
FAS	CSqS			
	MSqS			
	FSqS			
	NoS			

Table 15: Changes to the API / silica preblend feeding trials. Tests marked with "InC" were found to be incompatible

KT20		API & Silica Blend		
		80%	100%	125%
CCS	CSqS	X	X	X
	MSqS	X	X	X
	FSqS	InC	InC	InC
	NoS	X	X	X
CAS	CSqS	X	X	X
	MSqS	X	X	X
	FSqS	InC	InC	InC
	NoS	X	X	X
FCS	CSqS			
	MSqS			
	FSqS			
	NoS			
FAS	CSqS			
	MSqS			
	FSqS			
	NoS			